

IaaS Procurement by Simulated Annealing

Nader Alfares, Ata Fatahi Baarzi, George Kesidis
Pennsylvania State University
{nna5040,azf82,gik2}@psu.edu

Aman Jain
Microsoft
aman.jain@microsoft.com

July 12, 2022

Abstract

Considering the problem of resource allocation for potentially complex and diverse streaming (e.g., query processing) or long-running iterative (e.g., deep learning) workloads in the public cloud, we argue that a framework based on simulated annealing is suitable for navigating performance/cost trade-offs when selecting from among heterogeneous service offerings. Annealing is particularly useful when the complex workload and heterogeneous service offerings may vary over time. Based on a macroscopic objective that combines both performance and cost terms, annealing facilitates light-weight and coherent policies of exploration and exploitation when considering the service suite offered by a cloud provider. In this paper, we first give some background on simulated annealing and then demonstrate through experiments the usefulness of a particular resource management framework based on it: selecting the types and numbers of virtual machines for a particular job stream.

1 Introduction and Motivation

Resource management in the public cloud typically involves selecting available services spanning compute, storage and networking to minimize cost (or “cloud spend” [26]) subject to workload performance requirements, or a SLO to minimize cost subject to performance requirements. The problem is particularly challenging when serving a plurality of complex time-varying workloads. For a given set of job streams, the optimal service suite may involve a cluster composed of a variety of services. For example, a user can opt for Infrastructure-as-a-Service (IaaS) where virtual machines (VMs) are less costly per unit resource but slower to spin-up, and/or use Function-as-a-Service where cloud functions (CFs) are more costly per unit resource and may not be suitable for stateful applications but are faster to spin-up and are priced at a finer time granularity. Thus, VMs are preferred when reacting (autoscaling) to *sustained* changes in workload demand (e.g., predictions based on time-of-day) while CFs are preferred when reacting to rapid changes in demand [7, 15, 27].

Even within services of the same type resource instances can vary greatly. VMs can have different amounts and types of memory, CPU cores, hardware accelerators, and cross connects (e.g., PCIe, NVLink), and networking. Some VMs are cheaper because they provide only intermittent access to IT resources via token-bucket mechanisms [31] or can be revoked with timed notice [30]. Complicating matters further, some important resources are typically not virtualized (CPU cache, memory bandwidth), while the details behind other time-varying resources are not carefully spelled-out in the SLAs, e.g., bandwidth to local disk or remote storage [24] or token-bucket mechanisms governing access to CPU or network I/O [31]. In some cases, users can optionally pay to collocate VMs on the same physical server or to provision networking resources connecting their VMs to storage.¹ Given a procured service cluster, rules for scaling the cluster up or down, and a workload, critical decisions can dictate how individual tasks are defined and

¹There are similar efficient resource allocation challenges in “bare metal” and private data center scenarios where virtualized public-cloud services are not in play.

mapped to containerized services. Different task scheduling policies have been proposed e.g., [11,17,32,36]. and can be implemented on cluster managers such as Kubernetes (K8) [18, 28]. Alternatively or in combination, a microservice architecture based on replicated serverless functions can be used to realize some workloads [6,9,10,25], via platforms like OpenWhisk [2]. So, the mapping between a given workload and its optimal service suite is very complex (even if “default” task scheduling is used), and a typical user (cloud tenant) may provide little more guidance than “macroscopic” performance requirements (based on SLOs) and a cost budget.

A variety of approaches have been used toward managing performance and costs in the cloud for generic workloads. Some involve *using* deep learning to determine a service suite, scheduling tasks, etc. [5, 22, 25, 27]. However, deep learning is supervised requiring a very large curated training dataset representing a huge set of “exploratory” experiments for a given workload [13]. Changes to the workload (even to just the dataset on which it operates) or to the service suite (e.g., pricing described in the SLAs) may require adding “samples” to the training dataset and retraining the neural network, i.e., deep reinforcement learning [20]. Recently, researchers and practitioners have explored the use of more “traditional” and adaptable means of decision-making (including using model-based adaptive control, PID control, Markov decision processes) where artificial neural networks play only a partial role at most, e.g., [7,27,36]. In particular, some service procurement methods can operate both offline and online, i.e., they can make procurement decisions more dynamically. For example, genetic algorithms, e.g., [33,34], can be used to explore the service suite and dynamically react to changes in the workload and service offerings. But exploration under genetic algorithms is rather ad-hoc, sometimes involving significant changes to the current service suite.

In this paper, we take a simulated annealing approach (e.g., [1,12,16]) to the problem of provisioning an IaaS cluster for a plurality of different streaming workloads. Annealing works to minimize a macroscopic objective accounting for factors like current execution times and cost per unit time of the existing cluster. While it can operate both offline and online (runtime), our focus is on the latter. Under annealing, the degree of exploration versus exploitation is controlled by a single “temperature” parameter. Exploration is typically incremental (i.e., small changes to the cluster at a time) and can generally overcome local minima in the objective. To respond to changes in availability of services and/or the existing workload, the temperature can be dynamically increased resulting in more exploration. During a period of stable workload (demand), acceptable cost/performance trade-off, and fixed set of available services, the temperature can be slowly lowered to seek a global minimum of the objective (exploitation).

This paper is organized as follows. Some background on Spark and annealing is given in Section 2. A service procurement problem is formulated and an annealing based approach to it is described in Section 3. The results of a preliminary study are given in Section 4 using the Apache Spark distributed application and CloudLab. The paper concludes with a brief discussion of future work in Section 5.

2 Background

2.1 Apache Spark

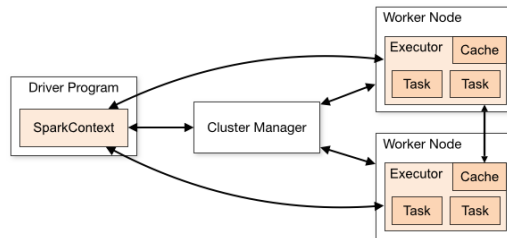


Figure 1: Apache Spark Architecture

Apache Spark [29,35] (or Spark) is an open source computing engine used for large-scale data processing applications. A typical Spark cluster setup consist of a single master and one or more workers. When a Spark application is submitted, a Spark driver is launched, which is the responsible component that requests for resources from the cluster manager (e.g., Mesos, YARN, Kubernetes or Spark’s Standalone cluster manager) as shown in Figure 1. Upon arrival of jobs, Spark schedules them in FIFO fashion, where each job is divided into map and reduce phases, also referred to as stages. These stages are represented as Directed Acyclic Graphs (DAG) i.e. a job’s execution plan generated by Spark. Executors are launched on worker nodes and tasks of each stage are sent to run on these executors. The memory size and number of cores assigned to executors can be modified through a configuration file when an application is submitted. Recent improvements have been made to Spark to better accommodate streaming applications, such as Flink [8].

2.2 Simulated Annealing - Overview

Simulated annealing was introduced in the 1980s, as a generic framework to minimize a complicated function $Y : D \rightarrow \mathbb{R}$ over continuous (uncountable) or very large discrete (countable) bounded domain D , where “complicated” means that Y has plural local minima in addition to global ones.

A *local* neighborhood function $\nu(x)$ for all $x \in D$ is defined, where $x \notin \nu(x)$. A collection of possible transitions between x and elements of $\nu(x)$ are also defined, often taken as all equally likely as assumed in the following (i.e., each with uniform probability $1/|\nu(x)|$). A key requirement of the neighborhood function ν is that it has to produce a connected graph². Typically, the neighborhood function ensures only *incremental* one-step changes to the current configuration state, but this is not a requirement.

Given Y, ν , one can define an annealing Markov chain on D at temperature $\tau > 0$ with transition probabilities from x to $x' \in \nu(x)$ being:

$$\frac{1}{|\nu(x)|} \exp\left(-\frac{\max\{Y(x') - Y(x), 0\}}{\tau}\right).$$

We see that a possible transition from the current state x to the next state x' is “accepted” with positive probability even when the objective Y is increased, i.e., when $Y(x') > Y(x)$, and always accepted when $Y(x') \leq Y(x)$ – this is the “heat bath” rule, e.g., [16]. When the temperature parameter τ increases, this acceptance probability increases, i.e., there is more exploration and less exploitation which is particularly useful when trying to avoid poor local minima. If the temperature τ is initially sufficiently high and slowly (logarithmically) decreases to zero over time, it can be shown that the (time-inhomogeneous) Markov chain Y will converge in probability to its global minimum on D [1]. But this limiting result is not very useful in practice. Even early on, some authors pointed out that it may be better not to thus “cool” the annealing chain [12], particularly when considering a finite time-horizon. If the temperature is fixed $\tau > 0$ and the neighborhoods all have the same size ($|\nu(x)|$ is a constant function of $x \in D$) then (time-homogeneous) Markov chain Y has (Gibbs) stationary distribution proportional to $\exp(Y(x)/\tau)$. Note that as the temperature $\tau \rightarrow 0$, only transitions when reduce Y are accepted, i.e., pure exploitation.

In the past, annealing was successfully applied to complex optimization problems such as placement and routing VSLI circuits and complex bin-packing problems [21]. Also, annealing can be combined with other optimization methods, e.g., where a memory of previously visited states and their performance is maintained like in Tabu search.

3 Problem Formulation and Annealing Approach

Consider a long job stream whose composition and workload profile may change periodically over time. This change could be due to changes in the types of jobs and their proportions and/or the datasets

²That is, the Markov chain resulting from the “base” transition probabilities associated with the neighborhood function is “irreducible”. These transition probabilities should be chosen so that the base Markov chain is also time-reversible [1].

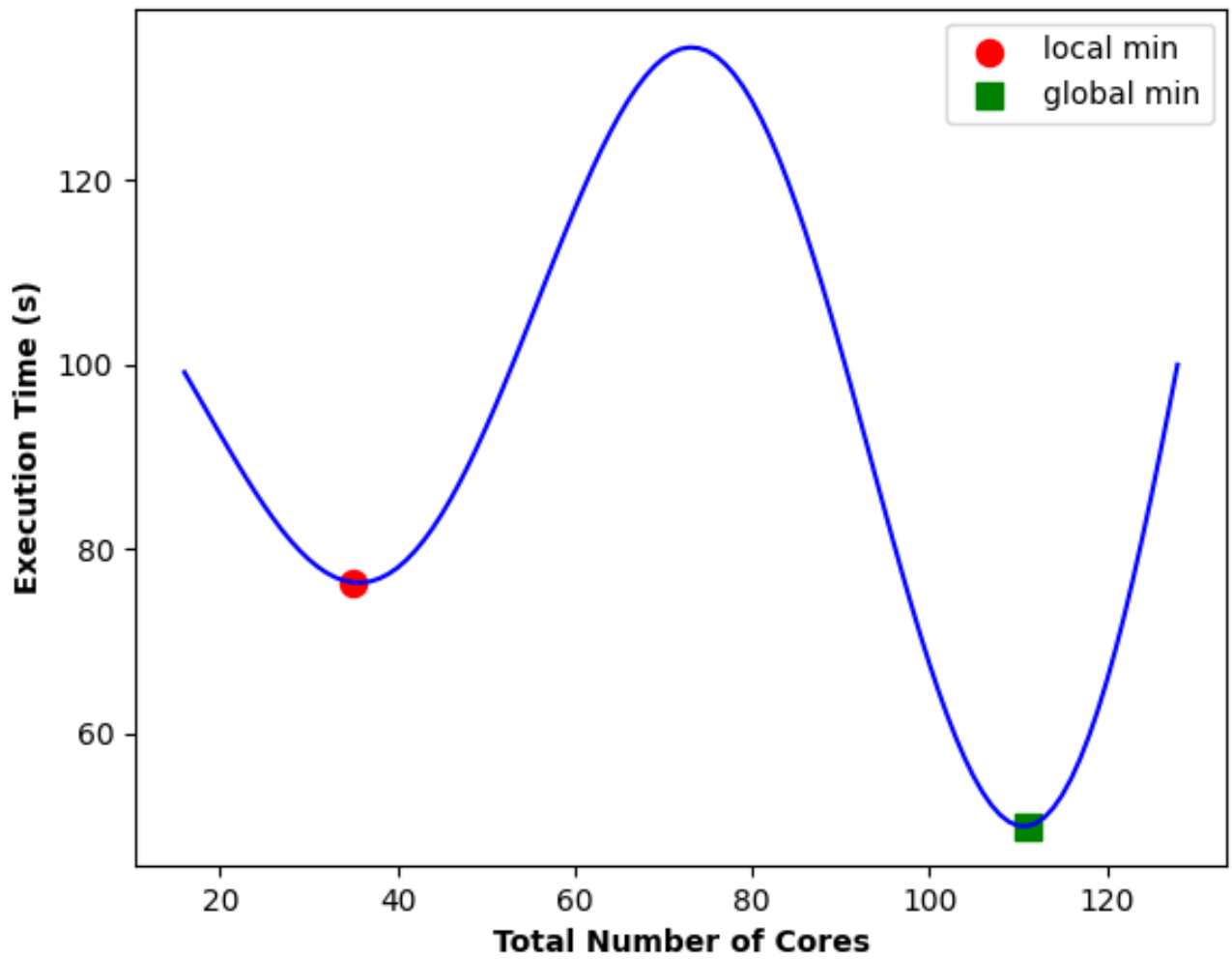


Figure 2: An illustrative example of an arbitrary workload characterizing the relationship between the total number of cores and the execution time. The green box and red circle mark minimums of execution times.

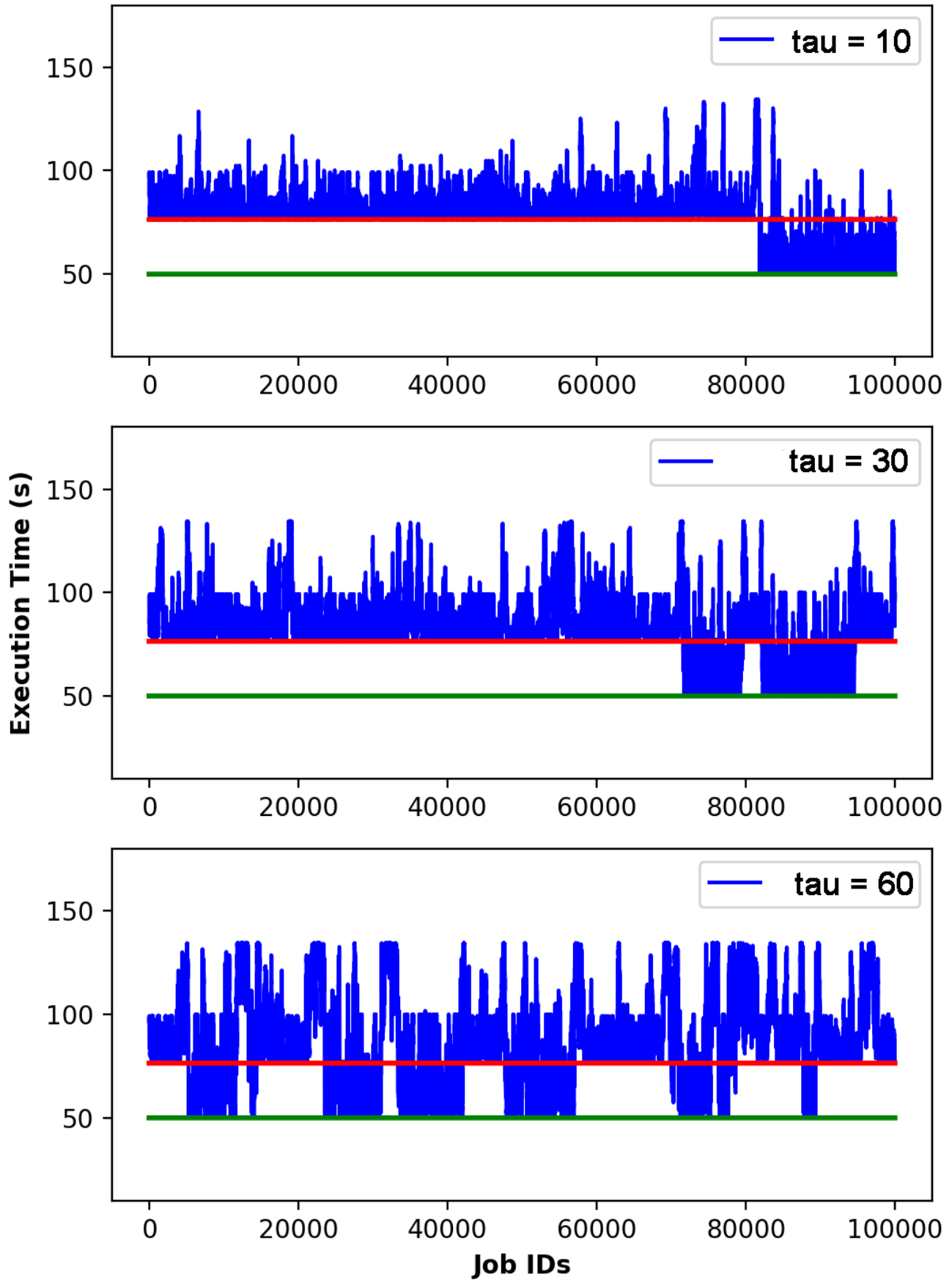


Figure 3: Simulating a stream of jobs submitted based on characteristics from figure 2. Both red and green lines represent the execution time at the minimums.

on which the jobs operate. The goal here is to decide on the most performance and cost effective IaaS cluster, including consideration of autoscaling costs, dynamic changes to the effective capacities and prices of services considered, or new service offerings.

First, consider a stream of the same type of job, e.g., the jobs are described by the same DAG of component tasks, for a fixed cluster. In addition, we assume that the size of the input dataset is the same for every job. Let x_k be the cluster configuration for the n^{th} job (e.g., indicating the total number of cores in the cluster). Starting with a random configuration for x_0 , we apply annealing over the course of the job stream with minimizing objective

$$Y_n = t_n + \lambda c_n$$

where t_n and c_n respectively are the total execution time and the cost for job n under the currently chosen service configuration. The user specified term $\lambda > 0$ weighs the cost against the execution time.

Second, we formulate the objective to be able to consider a blend of multiple types of jobs. The composition of the blended workload can be described using weighted averages of each type. For example, consider a workload that consists of N types of jobs. The minimizing objective for this workload can be described as the following: $Y = \sum_{i=1}^N \alpha^{(i)} Y^{(i)}$, where $\alpha^{(i)} > 0$ is the weight for workload i ($\sum_{i=1}^N \alpha^{(i)} = 1$), and $Y^{(i)}$ its objective to be minimized. The user specified parameter $\alpha^{(i)}$, which can be interpreted as the priority of workload i , may change dynamically as the workloads experience variations over time. Upon arrival of a new job (or new set of jobs) n , we run it (them) with the configuration z_n

$$z_n = x_{n-1} + e_v$$

where e_v represents a possible “step size” (incremental change) when exploring configurations and x_{n-1} represents the current “accepted” configuration. We set $x_n = z_n$ (i.e., accept the configuration z_n) with probability

$$\exp(-\max\{Y_n - Y_{n-1}, 0\}/\tau)$$

where Y_n is the objective evaluated for job n , and τ is a control parameter for either exploration and exploitation, otherwise $x_n = x_{n-1}$.

As an illustrative example, Figure 2 represents a one-dimensional characteristics of a single type of job. The red circle and green square depict the local and global minimums, respectively. In this example, the configuration that we want to optimize is the total number of cores used to run a job. For simplicity, we set the minimizing objective to be solely the total execution time of jobs (i.e., setting $\lambda = 0$ in the objective function above). We picked a bimodal distribution to illustrate that annealing can overcome a suboptimal local minimum (that is not global).

We simulate a stream of same-type jobs submitted, assuming that each job is executed independently (i.e., one job at a time). Figure 3 illustrates the execution time for each job submitted under simulated annealing with $e_v \in \{-1, 1\}$. We see that as the temperature τ increases (i.e., more exploration is done), simulated annealing reaches the global minimum (green line) more rapidly. Figure 4 depicts the number of jobs needed until a global minimum is found for the workload described in figure 2. Additionally, we find that as the temperature increases it takes fewer number of jobs to find the global minimum, i.e., more exploration than exploitation. Lastly, figure 5 illustrates how annealing can adapt to dynamic changes in the workload. Blue line resembles the workload characteristics show in figure 2, while orange line represents the new workload characterization after a sudden change. The bottom chart of figure 5 depicts execution time of different jobs being run under configuration provided by the annealing process. We can see that annealing can still find the new global minimum through its exploration phases, despite the change in the workload characteristics at the point depicted by the vertical red line.

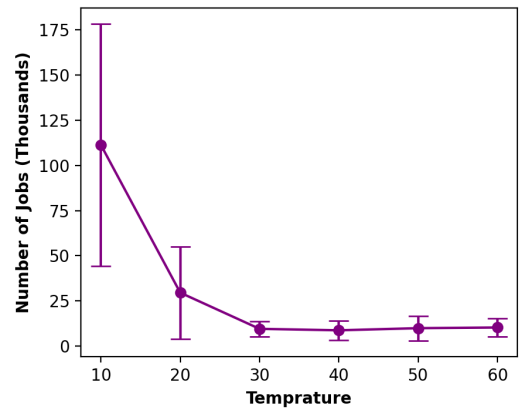


Figure 4: The number of jobs submitted before a configuration with the minimum objective is selected by the annealing process depends on the temperature. The vertical bars represent 95% confidence intervals (± 2 sample standard deviations).

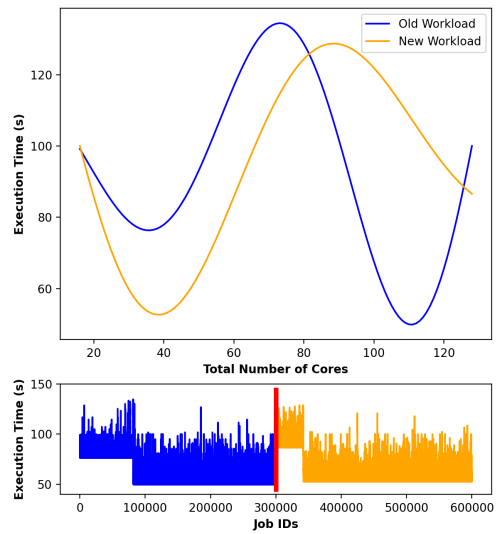
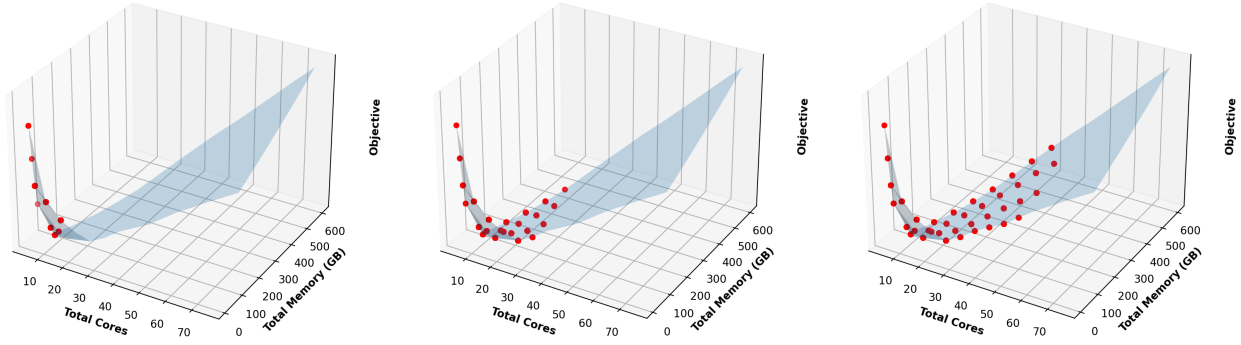


Figure 5: Workload changes in mid-operation. The red line in the bottom figure represents the change in workload characteristics.



(a) Low Temperature Annealing ($\tau = 10$) (b) Medium Temperature Annealing ($\tau = 25$) (c) High Temperature Annealing ($\tau = 50$)

Figure 6: Performing annealing on a blended workload of three types of jobs: Wordcount, K-means, and Pagerank

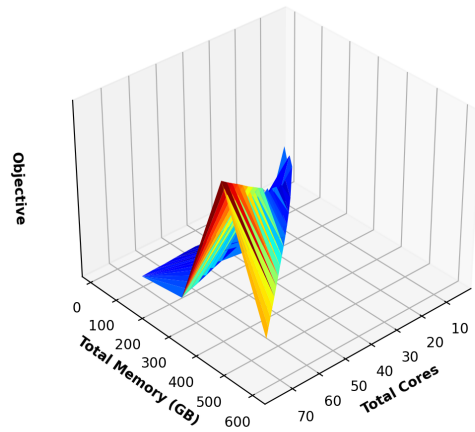


Figure 7: Blended workload characteristic based on four types of EC2 instances: General Purpose, Compute Optimized, Storage Optimized, and Memory Optimized.

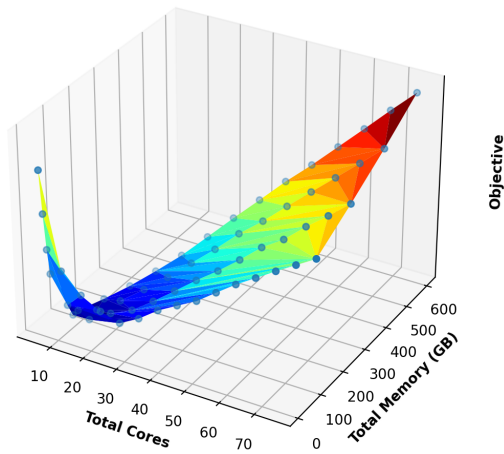


Figure 8: Blend of HiBench workload types (Wordcount, K-means and PageRank) with adjustment for storage-optimized instances for better comparisons.

4 Experimental Evaluation

4.1 Experimental Set-Up

We evaluate our simulated annealing approach using CloudLab [4] virtual machines. Our set-up consists of six nodes (a master node and 5 worker nodes). Each node consist of 40 core and 160 GB of memory. Using Apache Spark (3.1.2v), we exploit the Spark configuration file in the master node to set the new desired configuration when performing annealing.

4.2 Modeling Cost of EC2

We reference AWS’s EC2 per core pricing for different on-demand instance types. For each instance type, a pre-defined memory allocated per core is assumed (e.g., m6g.medium instances allocate 4 GB of memory per core procured). We also consider hypothetical instances “between” those offered by AWS with corresponding price adjustments (further details are given in section 4.2.1).

4.2.1 Each job executed independently

Using a blend of three different type of HiBench jobs [14], we evaluate the objective values, under different configurations, for the blended workload as described in section 3. We simulate a stream of independent jobs and record their average execution times under configurations provided by the annealing process, i.e., number of VM instances of a certain type where each VM type is characterized by a number of cores and memory allocated per core. Figure 7 depicts the objective values for different configurations of such blended workload. The peaks in figure 7 evaluates the objective values when using storage-optimized instances³. As presented previously in section 3, annealing can overcome local minima, especially at higher temperatures. Note that different ordering of the categorical instance types in defining the search space may introduce local minimums that are not global.

We replace the pricing of storage-optimized instances with a hypothetical family of instances for better comparisons (i.e., all families of instances have similar local storage performance) shown in figure 8. Figure 6 shows different simulations of jobs streams while performing annealing under different temperatures. The red dots represent different service-cluster configurations. From figures 6 and 9, we can observe that more exploration is performed by annealing as the temperature τ increases. Furthermore, figure 10 shows that as the temperature increases, the annealing process more quickly finds the configuration with the minimum objective, but with greater service variation due to higher service exploration.

4.2.2 Jobs executed in parallel

The annealing approach can also be employed for workloads that consist of jobs that are executed in parallel (i.e., when jobs compete for resources) and a job queue may be present. The minimizing objective can be adjusted for this case by measuring the sojourn time of jobs instead of execution times. The annealing process performs similarly to what is described in section 4.2.1. Hence, we leave out such experimental results to maintain conciseness.

4.3 Adaptation of Annealing

Similar to the illustrative example (section 3), we evaluate the adaptation of annealing for dynamic changes in the blended workload. Figure 11 shows the computed objective values for a stream of blended HiBench jobs. Here, we portray the change in workload as a change in the distribution of the blend (red vertical line depicts the point of time when the change occurs). The blue lines depict the objective

³Latency to local storage was not a significant performance factor in our experiments. Hence, AWS instances that use Elastic Block Store (EBS) are also emulated using SSDs, but with their actual AWS pricing.

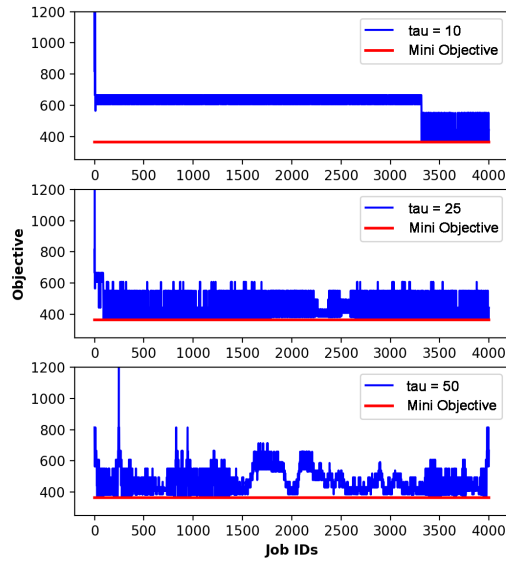


Figure 9: The occurrences of exploitation and exploration depends on the temperature. Each chart in the above represent performing an annealing process under a fixed temperature for a blended workload.

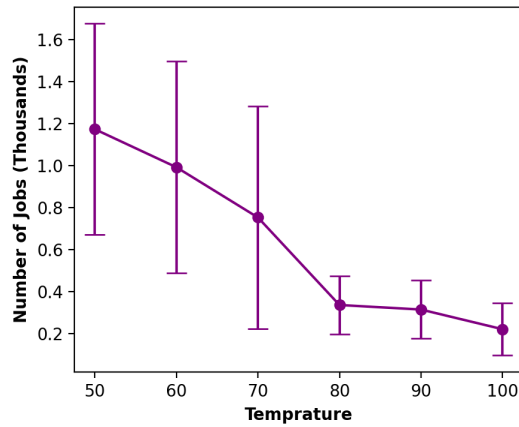


Figure 10: Similar to the illustrative example, the number of jobs submitted before a configuration with a minimum objective is selected depends on the temperature.

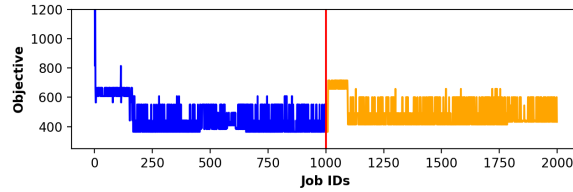


Figure 11: Annealing adapting to change in the blended Hibench workload.

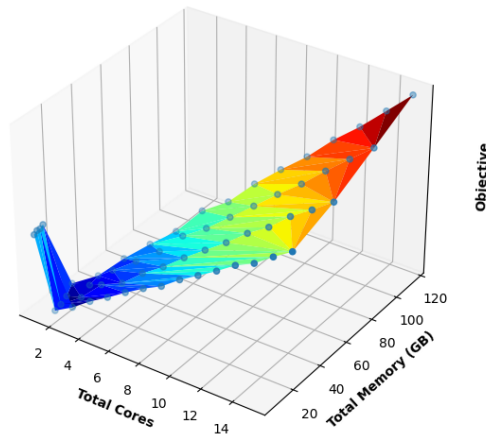


Figure 12: Training a Deep Neural Network using MNIST dataset for handwritten digits recognition.

values computed before the change occurs, while the orange lines depict after such. The oscillation in the computed objective values is due to the exploration nature of annealing at a positive temperature. After the change, we observe that annealing adapts to the change by finding the new objective-minimizing service configuration through exploration as well.

4.4 Deep Learning

The annealing method can also be utilized in training Deep Neural Networks (DNNs), i.e., deep learning. Figure 12 depicts the characterization of distributed deep learning, on our Spark cluster, using the Keras [3] library to build a Convolutional Neural Network (CNN) to recognize handwritten digits of the MNIST dataset [19]. Using the pricing model described in section 4.2, the goal is to find the service configuration that minimizes the objective function as described in section 3. The execution time here refers to training a model for one epoch. In our experiments, we set the initial configuration to 1 core with 4 GB of memory. Figure 13 shows the selected configurations that were explored by the annealing process (shown as red dots). From figure 14, we find that our annealing approach is capable of finding the configuration that minimizes the objective.

5 Future Work

The annealing approach can be easily extended to clusters of different types of services where the annealing state \underline{x} is simply a vector whose elements indicate the number of each service instance type currently in the cluster. One can also explicitly account for aspects of the input dataset that needs to be processed at each node, e.g., its size or domain specific features, like the mean and variance of the graph's degree distribution for PageRank.

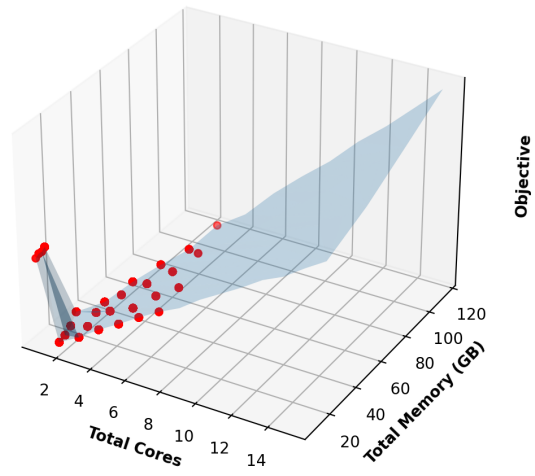


Figure 13: Performing Annealing on a Deep Neural Network using the MNIST dataset.

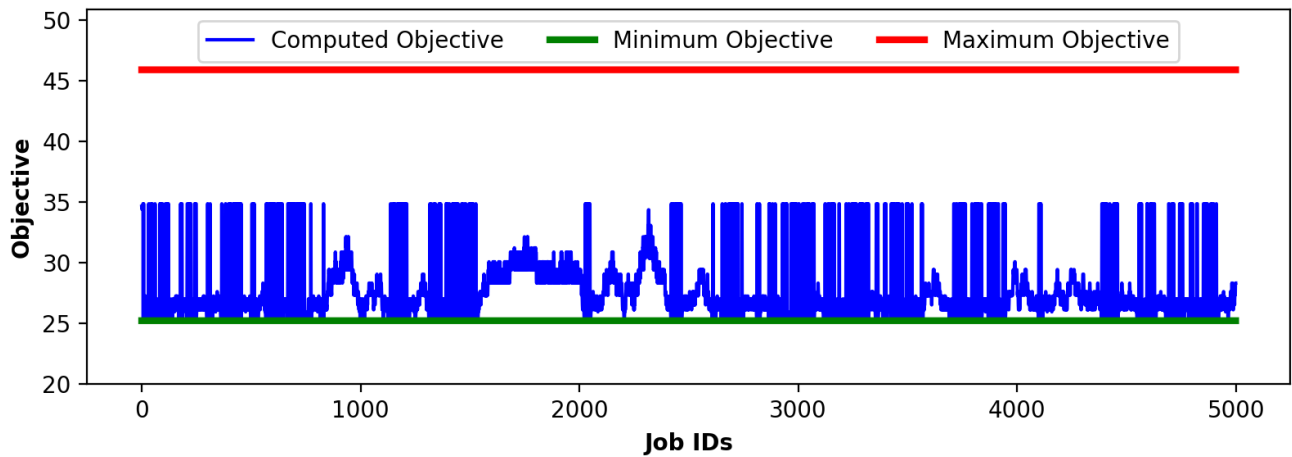


Figure 14: Computed objectives for selected configurations by the annealing process (blue line). The red and green lines correspond to configurations with the maximum and minimum objective values, respectively.

Previous studies have identified runtime causes of straggler tasks, e.g., execution stalls due to excessive CPU preprocessing and storage I/O delays [23], focusing on deep learning workloads, where such runtime diagnostics can involve artificial task-execution scenarios and datasets. These diagnostics lead to simple rules of thumb to address stragglers in future tasks of the same type which could in turn operate in concert with simulated annealing, e.g., to “force” a service-selection that likely has more available cores to a particular VM or container, especially if such a configuration has not been tried in the recent past. The annealing process would continue to run after such a move.

References

- [1] E. Aarts and J. Korst. *Simulated Annealing and Boltzmann Machines*. Wiley, 1989.
- [2] Apache OpenWhisk. <https://openwhisk.apache.org/>.
- [3] Francois Chollet and al. Keras. <https://github.com/fchollet/keras>, 2015.
- [4] Cloudlab. <https://www.cloudlab.us/>.
- [5] C. Delimitrou and C. Kozyrakis. HCloud: Resource-Efficient Provisioning in Shared Cloud Systems. In *Proc. ASPLOS*, 2016.
- [6] S. Eismann, M. Schwinger, J. Scheuner, J. Grohmann, E. van Eyk, N. Herbst, C.L. Abad, and A. Iosup. A Review of Serverless Use Cases and their Characteristics. Technical Report SPEC-RG-2020-5, Version 1.0, research.spec.org, 2020.
- [7] A. Fatahi and G. Kesidis. SHOWAR: Right-Sizing And Efficient Scheduling of Microservices. In *Proc. ACM SOCC*, Nov. 2021.
- [8] Apache Flink - Stateful Computations over Data Streams. <https://flink.apache.org/>.
- [9] Yu Gan, Yanqi Zhang, Dailun Cheng, Ankitha Shetty, Priyal Rathi, Nayantara Katarki, Ariana Bruno, Justin Hu, Brian Ritchken, Brendon Jackson, Kelvin Hu, Meghna Pancholi, Brett Clancy, Chris Colen, Fukang Wen, Catherine Leung, Siyuan Wang, Leon Zaruvinsky, Mateo Espinosa, Yuan He, and Christina Delimitrou. An Open-Source Benchmark Suite for Microservices and Their Hardware-Software Implications for Cloud and Edge Systems. In *Proceedings of the Twenty Fourth International Conference on Architectural Support for Programming Languages and Operating Systems (ASPLOS)*, April 2019.
- [10] Yu Gan, Yanqi Zhang, Kelvin Hu, Dailun Cheng, Yuan He, Meghna Pancholi, and Christina Delimitrou. Leveraging Deep Learning to Improve Performance Predictability in Cloud Microservices with Seer. *ACM SIGOPS Operating Systems Review*, 53(1), July 2019.
- [11] A. Ghodsi, M. Zaharia, B. Hindman, A. Konwinski, S. Shenker, and I. Stoica. Dominant resource fairness: Fair allocation of multiple resource types. In *Proc. USENIX NSDI*, 2011.
- [12] B. Hajek and G. Sasaki. Simulated annealing - to cool or not. *Systems and Control Letters*, 12(5):443–447, June 1989.
- [13] S. Higginbotham. Show Your Machine-Learning Work. *IEEE Spectrum*, Dec. 2019.
- [14] Shengsheng Huang, Jie Huang, Yan Liu, and Jinquan Dai. HiBench : A Representative and Comprehensive Hadoop Benchmark Suite. <https://www.intel.com/content/dam/develop/external/us/en/documents/hibench-wbdb2012-updated.pdf>, 2012.

- [15] A. Jain, A.F. Baarzi, N. Alfares, G. Kesidis, B. Urgaonkar, and M. Kandemir. SplitServe: Efficient Splitting Complex Workloads across FaaS and IaaS. In *Proc. ACM/IFIP Middleware*, Dec. 2020; *Proc. ACM SoCC* (extended abstract, poster presentation), Nov. 2019.
- [16] G. Kesidis and E. Wong. Optimal acceptance probability for simulated annealing. *Stochastics and Stochastics Reports*, Vol. 29:pp. 221–226, 1990.
- [17] J. Khamse-Ashari, I. Lambadaris, G. Kesidis, B. Urgaonkar, and Y.Q. Zhao. An Efficient and Fair Multi-Resource Allocation Mechanism for Heterogeneous Servers. *IEEE Trans. Parallel and Distributed Systems (TPDS)*, May 2018.
- [18] kube-scheduler. <https://kubernetes.io/docs/reference/command-line-tools-reference/kube-scheduler/>.
- [19] Y. Lecun, L. Bottou, Y. Bengio, and P. Haffner. Gradient-based learning applied to document recognition. *Proceedings of the IEEE*, 86(11):2278–2324, 1998.
- [20] Ning Liu, Zhe Li, Jielong Xu, Zhiyuan Xu, Sheng Lin, Qinru Qiu, Jian Tang, and Yanzhi Wang. A hierarchical framework of cloud resource allocation and power management using deep reinforcement learning. In *2017 IEEE 37th International Conference on Distributed Computing Systems (ICDCS)*, pages 372–382. IEEE, 2017.
- [21] Zhihong Liu, Qi Zhang, Mohamed Faten Zhani, Raouf Boutaba, Yaping Liu, and Zhenghu Gong. DREAMS: Dynamic resource allocation for MapReduce with data skew. In *IFIP/IEEE International Symposium on Integrated Network Management (IM)*, pages 18–26, 2015.
- [22] H. Mao, M. Schwarzkopf, S.B. Venkatakrisnan, Z. Meng, and M. Alizadeh. Learning scheduling algorithms for data processing clusters. <https://arxiv.org/pdf/1810.01963.pdf>.
- [23] J. Mohan, A. Phanishayee, A. Raniwala, and V. Chidambaram. Analyzing and mitigating data stalls in DNN training. In *Proc. VLDB*, Jan. 2021.
- [24] I. Pelle, J. Czentye, J.Doka, and B. Sonkoly. Towards latency sensitive cloud native applications: A performance study on AWS. In *Proc. IEEE CLOUD*, 2019.
- [25] H. Qiu, S.S. Banerjee, S. Jha, Z.T. Kalbarczyk, and R.K. Iyer. FIRM: An Intelligent Fine-grained Resource Management Framework for SLO-Oriented Microservices. In *Proc. OSDI*, 2020.
- [26] State of the cloud report: public cloud adoption grows as private cloud wanes. <https://www.rightscale.com/lp/state-of-the-cloud>, 2017.
- [27] K. Rzadca, P. Findeisen, J. Swiderski, P. Zych, P. Broniek, J. Kusmierk, P. Nowak, B. Strack, P. Witusowski, S. Hand, and J. Wilkes. Autopilot: Workload autoscaling at Google. In *Proc. ACM EuroSys*, 2020.
- [28] Scheduling Extensions in Kubernetes. <https://github.com/akanso/extending-kube-scheduler>, April, 25, 2021.
- [29] Spark. <http://spark.apache.org>, last accessed, Sept. 2017.
- [30] C. Wang, B. Urgaonkar, A. Gupta, G. Kesidis, and Q. Liang. Exploiting Spot and Burstable Instances for Improving the Cost-efficacy of In-Memory Caches on the Public Cloud. In *Proc. ACM EuroSys*, Belgrade, 2017.
- [31] C. Wang, B. Urgaonkar, N. Nasiriani, and G. Kesidis. Using Burstable Instances in the Public Cloud: When and How? In *Proc. ACM SIGMETRICS, Urbana-Champaign, IL*, June 2017.

- [32] W. Wang, B. Liang, and B. Li. Multi-resource fair allocation in heterogeneous cloud computing systems. *IEEE Transactions on Parallel and Distributed Systems*, 26(10):2822–2835, Oct. 2015.
- [33] David Wilcox, Andrew McNabb, and Kevin Seppi. Solving virtual machine packing with a reordering grouping genetic algorithm. In *Evolutionary Computation (CEC), 2011 IEEE Congress on*, pages 362–369. IEEE, 2011.
- [34] K. P. Wong and Y. W. Wong. Genetic and genetic/simulated-annealing approaches to economic dispatch. *IEEE Proc. Gener. Transm. Distrib.*, 141(5):507–513, 1994.
- [35] M. Zaharia, M. Chowdhury, M.J. Franklin, S. Shenker, and I. Stoica. Spark: Cluster Computing with Working Sets. In *Proc. USENIX HotCloud*, 2010.
- [36] H. Zhang, Y. Tang, A. Khandelwal, J. Chen, and I. Stoica. Caerus: Nimble Task Scheduling for Serverless Analytics. In *Proc. USENIX NSDI*, Apr. 2021.